First Observation of Self-Amplified Spontaneous Emission in a Free-Electron Laser at 109 nm Wavelength

J. Andruszkow,[16] B. Aune,[4] V. Ayvazyan,[27] N. Baboi,[10] R. Bakker,[2] V. Balakin,[3] D. Barni,[14] A. Bazhan,[3] M. Bernard,[21] A. Bosotti,[14] J. C. Bourdon,[21] W. Brefeld,[6] R. Brinkmann,[6] S. Buhler,[19] J.-P. Carneiro,[9] M. Castellano,[13] P. Castro,[6] L. Catani,[15] S. Chel,[4] Y. Cho,[1] S. Choroba,[6] E. R. Colby,[9,*] W. Decking,[6] P. Den Hartog,[1] M. Desmons,[4] M. Dohlus,[6] D. Edwards,[9] H. T. Edwards,[9] B. Faatz,[6] J. Feldhaus,[6] M. Ferrario,[13] M. J. Fitch,[26] K. Flöttmann,[6] M. Fouaidy,[19] A. Gamp,[6] T. Garvey,[21] C. Gerth,[6] M. Geitz,[10,†] E. Gluskin,[1] V. Gretchko,[17] U. Hahn,[6] W. H. Hartung,[9] D. Hubert,[6] M. Hüning,[24] R. Ischebek,[24] M. Jablonka,[4] J. M. Joly,[4] M. Juillard,[4] T. Junquera,[19] P. Jurkiewicz,[16] A. Kabel,[6,*] J. Kahl,[6] H. Kaiser,[6] T. Kamps,[7] V. V. Katelev,[12] J. L. Kirchgessner,[23] M. Körfer,[6] L. Kravchuk,[17] G. Kreps,[6] J. Krzywinski,[18] T. Lokajczyk,[6] R. Lange,[6] B. Leblond,[21] M. Leenen,[6] J. Lesrel,[19] M. Liepe,[10] A. Liero,[22] T. Limberg,[6] R. Lorenz,[7,‡] Lu Hui Hua,[11] Lu Fu Hai,[6] C. Magne,[4] M. Maslov,[12] G. Materlik,[6] A. Matheisen,[6] J. Menzel,[24] P. Michelato,[14] W.-D. Möller,[6] A. Mosnier,[4] U.-C. Müller,[6] O. Napoly,[4] A. Novokhatski,[5] M. Omeich,[21] H. S. Padamsee,[23] C. Pagani,[14] F. Peters,[6] B. Petersen,[6] P. Pierini,[14] J. Pflüger,[6] P. Piot,[6] B. Phung Ngoc,[4] L. Plucinski,[10] D. Proch,[6] K. Rehlich,[6] S. Reiche,[10,§] D. Reschke,[6] I. Reyzl,[6] J. Rosenzweig,[25] J. Rossbach,[6,**] S. Roth,[6] E. L. Saldin,[6] W. Sandner,[22] Z. Sanok,[8] H. Schlarb,[10] G. Schmidt,[6] P. Schmüser,[10] J. R. Schneider,[6] E. A. Schneidmiller,[6] H.-J. Schreiber,[7] S. Schreiber,[6] P. Schütt,[5] J. Sekutowicz,[6] L. Serafini,[14] D. Sertore,[6] S. Setzer,[5] S. Simrock,[6] B. Sonntag,[10] B. Sparr,[6] F. Stephan,[7] V. A. Sytchev,[12] S. Tazzari,[15] F. Tazzioli,[13] M. Tigner,[23] M. Timm,[5] M. Tonutti,[24] E. Trakhtenberg,[1] R. Treusch,[6] D. Trines,[6] V. Verzilov,[13] T. Vielitz,[6] V. Vogel,[3] G. v. Walter,[24] R. Wanzenberg,[6] T. Weiland,[5] H. Weise,[6] J. Weisend,[6,*] M. Wendt,[6] M. Werner,[6] M. M. White,[1] I. Will,[22] S. Wolff,[6] M. V. Yurkov,[20] K. Zapfe,[6] P. Zhogolev,[3] and F. Zhou[6,††]

[1]*Advanced Photon Source, Argonne National Laboratory, 9700 S. Cass Avenue, Argonne, Illinois 60439*
[2]*BESSY, Albert-Einstein-Strasse 15, 12489 Berlin, Germany*
[3]*Branch of the Institute of Nuclear Physics, 142284 Protvino, Moscow Region, Russia*
[4]*CEA Saclay, 91191 Gif-sur-Yvette, France*
[5]*Darmstadt University of Technology, FB18-Fachgebiet TEMF, Schlossgartenstrasse 8, 64289 Darmstadt, Germany*
[6]*Deutsches Elektronen-Synchrotron DESY, Notkestrasse 85, 22603 Hamburg, Germany*
[7]*Deutsches Elektronen-Synchrotron DESY, Platanenallee 6, 15738 Zeuthen, Germany*
[8]*Faculty of Physics and Nuclear Techniques, University of Mining and Metallurgy, al. Mickiewicza 30, PL-30-059 Cracow, Poland*
[9]*Fermi National Accelerator Laboratory, MS 306, P.O. Box 500, Batavia, Illinois 60510*
[10]*Hamburg University, Institut für Experimentalphysik, Notkestrasse 85, 20603 Hamburg, Germany*
[11]*Institute of High Energy Physics IHEP, FEL Laboratory, P.O. Box 2732, Beijing 100080, People's Republic of China*
[12]*Institute of High Energy Physics, 142284 Protvino, Moscow Region, Russia*
[13]*INFN-LNF, via E. Fermi 40, 00044 Frascati, Italy*
[14]*INFN Milano-LASA, via Fratelli Cervi 201, 20090 Segrate (MI), Italy*
[15]*INFN-Roma2, via della Ricerca Scientifica 1, 00100 Roma, Italy*
[16]*Institute of Nuclear Physics, Ul. Kawiory 26 a, 30-55 Krakow, Poland*
[17]*Institute for Nuclear Research of RAS, 117312 Moscow, 60th October Anniversary Prospect 7A, Russia*
[18]*Institute of Physics, Polish Academy of Sciences, al. Lotnikow, 32/46, 02-668 Warsaw, Poland*
[19]*Institut de Physique Nucléaire (CNRS-IN2P3), 91406 Orsay Cedex, France*
[20]*Joint Institute for Nuclear Research, 141980 Dubna, Moscow Region, Russia*
[21]*Laboratoire de l'Accélérateur Linéaire, IN2P3-CNRS, Université de Paris-Sud, B.P. 34, F-91898 Orsay, France*
[22]*Max-Born-Institute, Max-Born-Strasse 2a, 12489 Berlin, Germany*
[23]*Newman Lab, Cornell University, Ithaca, New York 14850*
[24]*RWTH Aachen-Physikzentrum, Physikalisches Institut IIIa, Sommerfeldstrasse 26-28, 52056 Aachen, Germany*
[25]*UCLA Department of Physics and Astronomy, 405 Hilgard Ave., Los Angeles, California 90095*
[26]*University of Rochester, Department of Physics and Astronomy, 206 Bausch & Lomb, Rochester, New York 14627*
[27]*Yerevan Physics Institute, 2 Alikhanyan Brothers Street, 375036 Yerevan, Armenia*

(Received 17 April 2000)

We present the first observation of self-amplified spontaneous emission (SASE) in a free-electron laser (FEL) in the vacuum ultraviolet regime at 109 nm wavelength (11 eV). The observed free-electron laser gain (approximately 3000) and the radiation characteristics, such as dependency on bunch charge, angular distribution, spectral width, and intensity fluctuations, are all consistent with the present models for SASE FELs.

0031-9007/00/85(18)/3825(5)$15.00 © 2000 The American Physical Society

PACS numbers: 41.60.Cr, 29.17.+w, 29.27.–a, 52.75.Va

X-ray lasers are expected to open up new and exciting areas of basic and applied research in biology, chemistry, and physics. Because of recent progress in accelerator technology, the attainment of the long-sought-after goal of wide-range tunable laser radiation in the vacuum ultraviolet (VUV) and x-ray spectral regions is coming close to realization with the construction of free-electron lasers (FELs) [1] based on the principle of self-amplified spontaneous emission (SASE) [2,3]. In a SASE FEL, lasing occurs in a single pass of a relativistic, high-quality electron bunch through a long undulator magnet structure.

The radiation wavelength λ_{ph} of the first harmonic of FEL radiation is related to the period length λ_u of a planar undulator by

$$\lambda_{\mathrm{ph}} = \frac{\lambda_u}{2\gamma^2}\left(1 + \frac{K^2}{2}\right), \tag{1}$$

where $\gamma = E/(m_e c^2)$ is the relativistic factor of the electrons, $K = eB_u\lambda_u/(2\pi m_e c)$ is the undulator parameter, and B_u is the peak magnetic field in the undulator. Equation (1) exhibits two main advantages of the free-electron laser: (i) the free tunability of the wavelength by changing the electron energy and (ii) the possibility to achieve very short radiation wavelengths.

For most FELs presently in operation [4], the electron beam quality and the undulator length result in a gain of only a few percent per undulator passage, so that an optical cavity resonator and a synchronized multibunch electron beam have to be used. At very short wavelengths, normal-incidence mirrors of high reflectivity are unavailable. Therefore the generation of an electron beam of extremely high quality in terms of emittance, peak current, and energy spread, and a high precision undulator of sufficient length are essential. Provided the spontaneous radiation from the first part of the undulator overlaps the electron beam, the electromagnetic radiation interacts with the electron bunch leading to a density modulation (microbunching) which enhances the power and coherence of radiation. In this "high-gain mode" [5–7], the radiation power $P(z)$ grows exponentially with the distance z along the undulator

$$P(z) = AP_{\mathrm{in}}\exp(2z/L_g), \tag{2}$$

where L_g is the field gain length, P_{in} is the effective input power (see below), and A is the input coupling factor [6,7]. A is equal to $1/9$ in one-dimensional FEL theory with an ideal electron beam.

Since at short wavelengths there is no tunable laser to provide the input power P_{in}, the spontaneous undulator radiation from the first part of the undulator is used as an input signal to the downstream part. Typical parameters for a SASE FEL operating in the VUV wavelength range are P_{in} of about a few watts and power gain at saturation, $G = P_{\mathrm{sat}}/P_{\mathrm{in}}$, of about 10^8. Compared to state-of-the-art synchrotron radiation sources, one expects full transverse coherence, up to 4–6 orders of magnitude larger average brilliance, and up to 8–10 orders of magnitude larger peak brilliance at pulse lengths of about 200 fs FWHM [8–11] (brilliance defined as photon spectral density per unit time per unit radiating area per unit solid angle). Recently there have been important advances in demonstrating a high-gain SASE FEL at 12 μm wavelength [12] and at 530 nm wavelength [13].

The experimental results presented in this paper have been achieved at the TESLA Test Facility (TTF) free-electron laser [14] at the Deutsches Elektronen-Synchrotron DESY. The TESLA (TeV Energy Superconducting Linear Accelerator) collaboration consists of 39 institutes from 9 countries and aims at the construction of a 500 GeV (center-of-mass) e^+e^- linear collider with an integrated x-ray laser facility [10]. Major hardware contributions to TTF have come from Germany, France, Italy, and the USA. The goal of the TTF FEL is to demonstrate SASE FEL emission in the VUV and, in a second phase, to build a soft x-ray user facility [15,16]. The layout is shown in Fig. 1. The main parameters for FEL operation are compiled in Table I.

The injector is based on a laser-driven $1\frac{1}{2}$-cell rf gun electron source operating at 1.3 GHz [17]. The Cs_2Te cathode [18] is illuminated by a train of UV laser pulses generated in a mode-locked solid-state laser system [19] synchronized with the rf. The laser pulse length measured with a streak camera is $\sigma_t = 7.1 \pm 0.6$ ps. The superconducting accelerator structure has been described elsewhere [20].

The undulator is a fixed 12 mm gap permanent magnet device using a combined function magnet design [21] with a period length of $\lambda_u = 27.3$ mm and a peak field of $B_u = 0.46$ T, resulting in an undulator parameter of $K = 1.17$. The beam pipe diameter in the undulator (9.5 mm) [22] is much larger than the beam diameter (300 μm). Integrated quadrupole structures produce a gradient of 12 T/m superimposed on the periodic undulator field in order to focus the electron beam along the undulator. The undulator system is subdivided into three segments, each 4.5 m long and containing 10 quadrupole sections to build

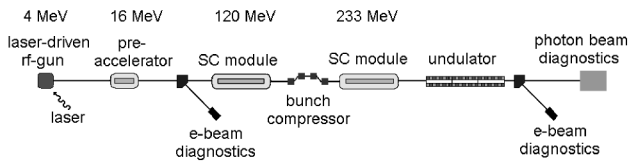


FIG. 1. Schematic layout of phase 1 of the SASE FEL at the TESLA Test Facility at DESY, Hamburg. The linac contains two 12.2 m long cryogenic modules each equipped with eight 9-cell superconducting accelerating cavities [20]. The total length is 100 m.

TABLE I. Main parameters of the TESLA Test Facility for FEL experiments (TTF FEL, phase 1).

Parameter	Measured value
Beam energy	233 ± 5 MeV
rms energy spread	0.3 ± 0.2 MeV
rms transverse beam size	100 ± 30 μm
Normalized emittance, ε_n	6 ± 3π mrad mm
Electron bunch charge	1 nC
Peak electron current	400 ± 200 A
Bunch spacing	1 μs
Repetition rate	1 Hz
Undulator period, λ_u	27.3 mm
Undulator peak field	0.46 T
Effective undulator length	13.5 m
Avg. betatron function horizontal/vertical	1.2 m/1.1 m
Radiation wavelength, λ_{ph}	109 nm
FEL gain	3×10^3
FEL radiation pulse length	0.4–1 ps

up 5 full focusing-defocusing periods. There is a spacing of 0.3 m between adjacent segments for diagnostics. The total length of the system is 14.1 m.

Beam orbit straightness in the undulator is necessary for optimum overlap between the electron and light beams. It is determined by the alignment precision of the superimposed permanent-magnet quadrupole fields which is better than 50 μm in both vertical and horizontal directions [23].

Different techniques have been used to measure the emittance of the electron beam [24] and yield values for the normalized emittance of $(4 \pm 1)\pi$ mrad mm for a bunch charge of 1 nC at the exit of the injector. The emittance in the undulator was typically between 6 and 10π mrad mm (in both horizontal and vertical phase space). It should be noted that the measurement techniques applied determine the emittance integrated over the entire bunch length. However, for FEL physics, the emittance of bunch slices much shorter than the bunch length is the relevant parameter. It is likely that, due to spurious dispersion and wakefields, the bunch axis is tilted about a transverse axis such that the projected emittance is larger than the emittance of any slice. Based on these considerations we estimate the normalized slice emittance in the undulator at $(6 \pm 3)\pi$ mrad mm.

A bunch compressor is inserted between the two accelerating modules, in order to increase the peak current of the bunch up to $\hat{I} = 500$ A. For a longitudinal charge distribution with Gaussian density profile and total charge of $Q = 1$ nC, such a peak current corresponds to a standard deviation (i.e., rms) of the bunch length of $\sigma_s = Qc/(\sqrt{2\pi}\,\hat{I}) = 0.24$ mm or to an rms pulse length of $\sigma_t = \sigma_s/c = 0.8$ ps. Experimentally, it is routinely verified that a large fraction of the bunch charge is compressed to a length below 0.4 mm (rms) [25]. There are indications that the core is compressed even further. We estimate the peak current for the FEL experiment at (400 ± 200) A.

For radiation intensity measurements we used a PtSi photodiode integrating over all wavelengths. The detector unit was placed 12 m downstream from the undulator exit. A 0.5 mm iris was placed in front of the photodiode in order to avoid saturation effects.

Strong evidence for the FEL process is a large increase in the on-axis radiation intensity if the electron beam is injected such that it overlaps with the radiation during the entire passage through the undulator. The observed intensity inside a window of ±200 μm around the optimum beam position was enhanced by a factor of more than 100 compared to the intensity of spontaneous radiation observed outside this window.

SASE gain is expected to depend on the bunch charge in an extremely nonlinear way. Figure 2 shows the measured intensity on axis as a function of bunch charge Q, while the beam orbit is kept constant for optimum gain. The solid line indicates the intensity of the spontaneous undulator radiation multiplied by a factor of 100. The strongly nonlinear increase of the intensity as a function of bunch charge is definite proof of FEL action. The gain does not further increase if the bunch charge exceeds some 0.6 nC. This needs further study, but it is known that the beam emittance becomes larger for increasing Q, thus reducing the FEL gain.

The wavelength spectrum of the radiation (taken on axis at maximum FEL gain) is presented in Fig. 3. The central wavelength of 108.5 nm is consistent with the measured beam energy of (233 ± 5) MeV and the known undulator parameter $K = 1.17$ [see Eq. (1)]. The intensity gain determined with the CCD camera of the spectrometer is in agreement with the photodiode result.

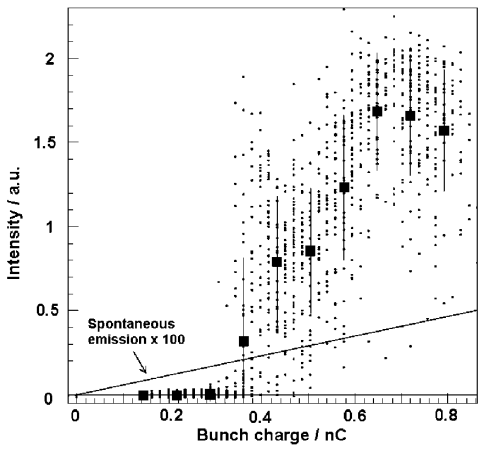


FIG. 2. SASE intensity versus bunch charge. The straight line is the spontaneous intensity multiplied by a factor of 100. To guide the eye, mean values of the radiation intensity are shown for some bunch charges (dots). The vertical error bars indicate the standard deviation of intensity fluctuations, which are due to the statistical character of the SASE process [see Eq. (3)].

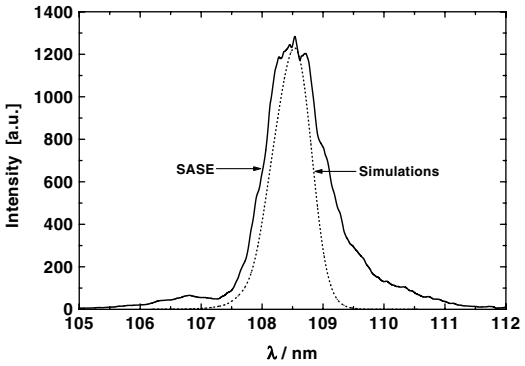


FIG. 3. Wavelength spectrum of the central radiation cone (collimation angle ± 0.2 mrad), taken at maximum FEL gain. The dotted line is the result of numerical simulation. The bunch charge is 1 nC.

A characteristic feature of SASE FELs is the concentration of radiation power into a cone much narrower than that of wavelength integrated undulator radiation, whose opening angle is on the order of $1/\gamma$. Measurements done by moving the 0.5 mm iris horizontally together with the photodiode confirm this expectation (see Fig. 4). To be visible on this scale, the spontaneous intensity is amplified by a factor of 30. The energy flux is 2 nJ/mm^2 at the location of the detector, and the on-axis flux per unit solid angle is about 0.3 J/sr (assuming a source position at the end of the undulator). This value was used as a reference point for the numerical simulation of the SASE FEL with the code FAST [26]. The longitudinal profile of the bunch current was assumed to be Gaussian with an rms length of 0.25 mm. The transverse distribution of the beam current density was also taken to be Gaussian. Calculations have been performed for a Gaussian energy spread of 0.1% and the normalized emittance ε_n was varied in the simulations between 2 and 10π mrad mm. Our calculations show that in this range of parameters the value of the effective power of shot noise P_{in} and coupling factor $A \simeq 0.1$ [see Eq. (2)] are nearly constant. A level of energy flux of 0.3 J/sr is obtained at five field gain lengths L_g. With these parameters the FEL gain can be estimated at $G \approx 3 \times 10^3$ with a factor of 3 uncertainty (i.e., $10^3 < G < 10^4$) which is mainly due to the imprecise knowledge of the longitudinal beam profile. If we assume that the entire undulator contributes to the FEL amplification process, we estimate the normalized emittance ε_n at 8π mrad mm, in reasonable agreement with the measurements. This value of the emittance was used for more detailed calculations of the FEL characteristics. Figures 3 and 4 include typical theoretical spectral and angular distributions. In both cases the experimental curves are wider than the simulation results. A possible source of the widening is energy and orbit jitter, since the experimental curves are the results of averaging over many bunches.

It is essential to realize that the fluctuations seen in Fig. 2 are not primarily due to unstable operation of the accelerator but are inherent to the SASE process. Shot noise in the electron beam causes fluctuations of the beam density, which are random in time and space [27]. As a result, the radiation produced by such a beam has random amplitudes and phases in time and space, and can be described in terms of statistical optics. In the linear regime of a SASE FEL, the radiation pulse energy is expected to fluctuate according to a gamma distribution $p(E)$ [28],

$$p(E) = \frac{M^M}{\Gamma(M)} \left(\frac{E}{\langle E\rangle}\right)^{M-1} \frac{1}{\langle E\rangle} \exp\left(-M\,\frac{E}{\langle E\rangle}\right), \quad (3)$$

where $\langle E\rangle$ is the mean energy, $\Gamma(M)$ is the gamma function with argument M, and $M^{-1} = \langle (E - \langle E\rangle)^2\rangle / \langle E\rangle^2$ is the normalized variance of E. The parameter M corresponds to the number of optical modes. Note that the same type of statistics applies for completely chaotic polarized light, in particular for spontaneous undulator radiation.

For our statistical measurements the signals from 3000 radiation pulses have been recorded, with the small iris (0.5 mm diam) in front of the photodiode to guarantee that

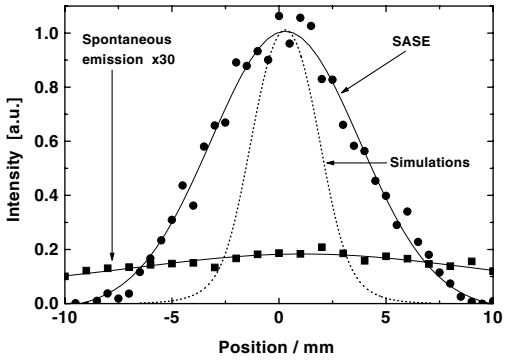


FIG. 4. Horizontal intensity profile of SASE FEL and spontaneous undulator radiation ($\times 30$), measured with a photodiode behind a 0.5 mm aperture in a distance of 12 m from the end of the undulator. The dotted line is the result of numerical simulation.

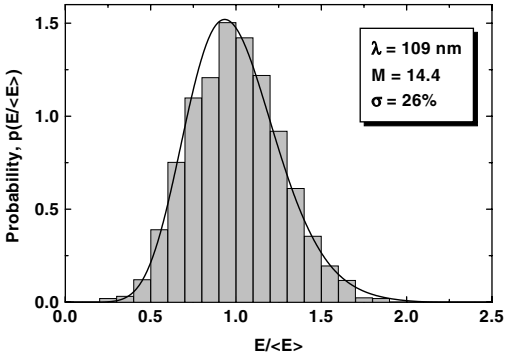


FIG. 5. Probability distribution of SASE intensity. The rms fluctuation yields a number of longitudinal modes $M = 14$. The solid curve is the gamma distribution for $M = 14.4$. The bunch charge is 1 nC.

transversely coherent radiation pulses are selected. Thus, the parameter M corresponds to the number of longitudinal modes. As one can see from Fig. 5, the distribution of the energy in the radiation pulses is quite close to the gamma distribution. The relative rms fluctuations are about 26% corresponding to $M = 14.4$. One should take into account the fact that these fluctuations arise not only from the shot noise in the electron beam; the pulse-to-pulse variations of the beam parameters can also contribute to the fluctuations. Thus, the value $M \approx 14$ can be considered as a lower limit for the number of longitudinal modes in the radiation pulse. By using the standard deviation of the radiation spectrum $\sigma_{\Delta\lambda/\lambda} = 0.36\%$, we calculate the coherence time [28] according to $\tau_{\mathrm{coh}} = \sqrt{\pi}/(\sigma_{\Delta\lambda/\lambda}\omega_{\mathrm{ph}}) = 28$ fs (with $\omega_{\mathrm{ph}} = 2\pi c/\lambda_{\mathrm{ph}}$) and find that the part of the electron bunch contributing to the SASE process is at least $Mc\tau_{\mathrm{coh}} \approx 120$ μm long. From the quality of the agreement with the gamma distribution we can also conclude that the statistical properties of the radiation are described with Gaussian statistics. In particular, this means that there are no FEL saturation effects.

The authors are deeply indebted to the late Bjørn H. Wiik who initiated and continuously supported the FEL activities at DESY. Fundamental work on high accelerating gradients in superconducting cavities at Wuppertal University was essential for the successful construction of the first TTF accelerating modules. We are grateful for the invaluable support by the technical staff of the participating groups. Support by the Moscow Physical Engineering Institute and by the Institute for Nuclear Studies, Swierk, Poland, is gratefully acknowledged.

*Present address: Stanford Linear Accelerator Center, SLAC MS 07, 2575 Sand Hill Road, Menlo Park, CA 94025.
†Present address: Procter & Gamble, 53881 Euskirchen, Germany.
‡Present address: Senderbetriebstechnik Westdeutscher Rundfunk, 50600 Köln, Germany.
§Present address: UCLA Department of Physics & Astronomy, Los Angeles, CA 90024.
**Email address: joerg.rossbach@desy.de
††Present address: CERN, CH 1211 Geneva 23, Switzerland.

[1] J. M. J. Madey, J. Appl. Phys. **42**, 1906 (1971).
[2] A. M. Kondratenko and E. L. Saldin, Part. Accel. **10**, 207 (1980).
[3] R. Bonifacio, C. Pellegrini, and L. M. Narducci, Opt. Commun. **50**, 373 (1984).
[4] W. B. Colson, Nucl. Instrum. Methods Phys. Res., Sect. A **429**, 37 (1999).
[5] K. J. Kim, Phys. Rev. Lett. **57**, 1871 (1986).
[6] S. Krinsky and L. H. Yu, Phys. Rev. A **35**, 3406 (1987).
[7] E. L. Saldin, E. A. Schneidmiller, and M. V. Yurkov, *The Physics of Free Electron Lasers* (Springer, New York, 1999), and references therein.
[8] H. Winick *et al.,* in PAC Proceedings, Washington, 1993 (unpublished); Report SLAC-PUB-6185.
[9] R. Brinkmann *et al.,* Nucl. Instrum. Methods Phys. Res., Sect. A **393**, 86 (1997).
[10] DESY Report 1997-048, edited by R. Brinkmann, G. Materlik, J. Rossbach, and A. Wagner, 1997; ECFA Report 1997-182, 1997.
[11] H.-D. Nuhn and J. Rossbach, Synchrotron Radiation News **13**, No. 1, 18 (2000).
[12] M. Hogan *et al.,* Phys. Rev. Lett. **81**, 4867 (1998).
[13] S. Milton *et al.,* Phys. Rev. Lett. **85**, 988 (2000).
[14] W. Brefeld *et al.,* Nucl. Instrum. Methods Phys. Res., Sect. A **393**, 119 (1997).
[15] T. Åberg *et al.,* A VUV FEL at the TESLA Test Facility at DESY (Conceptual Design Report) DESY Report TESLA-FEL 95-03, 1995.
[16] J. Rossbach, Nucl. Instrum. Methods Phys. Res., Sect. A **375**, 269 (1996).
[17] J.-P. Carneiro *et al.,* in Proceedings of the 1999 IEEE Particle Accelerator Conference, New York, IEEE Catalog No. 99CH36366, ISBN 0-7803-5573-3, 1999, pp. 2027–2029 (unpublished).
[18] P. Michelato *et al.,* Nucl. Instrum. Methods Phys. Res., Sect. A **445**, 422 (2000).
[19] S. Schreiber *et al.,* Nucl. Instrum. Methods Phys. Res., Sect. A **445**, 427 (2000).
[20] H. Weise, in *Proceedings of the 1998 Linac Conference, Chicago* (Report ANL-98/28) (Argonne National Lab., Chicago, 1998), p. 674.
[21] Y. M. Nikitina and J. Pflüger, Nucl. Instrum. Methods Phys. Res., Sect. A **375**, 325 (1996).
[22] U. Hahn *et al.,* Nucl. Instrum. Methods Phys. Res., Sect. A **445**, 442 (2000).
[23] J. Pflüger, Nucl. Instrum. Methods Phys. Res., Sect. A **445**, 366 (2000).
[24] H. Edwards *et al.,* in *Proceedings of the 1999 FEL Conference, Hamburg* (North-Holland, Amsterdam, 2000), II-75.
[25] M. Geitz, G. Schmidt, P. Schmüser, and G. V. Walter, Nucl. Instrum. Methods Phys. Res., Sect. A **445**, 343 (2000).
[26] E. L. Saldin, E. A. Schneidmiller, and M. V. Yurkov, Nucl. Instrum. Methods Phys. Res., Sect. A **429**, 233 (1999).
[27] R. Bonifacio *et al.,* Phys. Rev. Lett. **73**, 70 (1994).
[28] E. L. Saldin, E. A. Schneidmiller, and M. V. Yurkov, Opt. Commun. **148**, 383 (1998).